ELSEVIER

Carbohydrate Research 300 (1997) 31–40

CARBOHYDRATE RESEARCH

Structural characterization of organized systems of polysaccharides and phospholipids by light scattering spectroscopy and electron microscopy

Nuno C. Santos [a,b], Adelaide M.A. Sousa [a], Didier Betbeder [c], Manuel Prieto [a], Miguel A.R.B. Castanho [a,b,*]

[a] *Centro de Química-Física Molecular, Instituto Superior Técnico, 1096 Lisboa Codex, Portugal*
[b] *Dep. de Química e Bioquímica, Faculdade de Ciências da Universidade de Lisboa, Edifício C1, Campo Grande, 1700 Lisboa, Portugal*
[c] *Biovector Therapeutics, S.A., Chemin du Chêne Vert, 31676 Labège Cedex, France*

Received 1 August 1996; accepted 17 December 1996

Abstract

Biovectors are recently developed nanoparticles intended to be used as drug carriers and in the formulation of vaccines. The Biovectors are composed of a polysaccharide core to which phospholipids and cholesterol can be added. The cores are prepared by disruption of a gel of cross-linked maltodextrins, and can have a positive, neutral or negative charge depending on the grafting ionic ligands used. In this study static and dynamic light scattering measurements were combined to characterize the structure of these Biovectors. Transmission electron microscopy was also used. The present work, carried out with positively charged Biovectors in PBS (phosphate buffer saline) and phosphate buffer, points towards a microgel like structure to the polysaccharide fragments of these Biovectors and a spherical geometry with radius ≈ 50 nm. The influence of lipid composition on Biovectors size and density was also studied. The use of transmission electron microscopy gives first evidence for a structure consisting of several phospholipid bilayers surrounding a polysaccharide core. This organized lipidic environment is suitable for hydrophobic drug interaction and membrane proteins insertion. The formulation of a stable, highly controlled drug delivery system or vaccine formulation is implicated. © 1997 Elsevier Science Ltd.

Keywords: Drug carrier; Vaccine; Maltodextrin; Light scattering; Nanoparticle; Microgel

1. Introduction

A new family of polysaccharide/phospholipids systems intended for therapeutic use as drug delivery systems or vaccine formulations — Biovectors — has been recently developed. Biovectors are prepared from polysaccharide gel fragments obtained by disruption of a gel of chemically cross-linked maltodextrins in a Rannie homogenizer (APV, France). These cores can be neutral, or positively or negatively charged, depending on the meshing agent and/or

* Corresponding author. Fax: +351-1-3524372; e-mail: pcmcastanho@alfa.ist.utl.pt.

PII S0008-6215(97)00025-6

additional charged groups used for the synthesis. These nanoparticles are subsequently phospholipidated with, e.g., DPPC (dipalmitoylphosphatidylcholine) or EYPC (egg yolk phosphatidylcholine). Cholesterol can also be added.

Liposomes, the most popular among all artificial lipid based systems, have gained acceptance as potential drug carriers but present several basic problems that still remain to be solved for their biological or medical use (e.g., [1]). These include the low entrapment capability and the rapid uptake by phagocytic cells in the liver and spleen (e.g., [2]). Greater stability of a carrier is another of the goals that need to be achieved when considering in vivo administration.

The originality of Biovectors is to combine the possibility of carrying ionic drugs to the polysaccharide core and lipid or amphiphilic compounds in the membrane [3]. The main component of these vectors, maltodextrin, has a stable structure, is biologically inert and biodegradable and, more important, it possess many hydroxyl groups allowing chemical grafting of other molecules. This means that besides presenting no significative immune response [4] and no toxic side effects, Biovectors should enable the entrapment of specific drugs [3]. Based on important results on the structural stabilization of membranes against dryness and freezing achieved by the presence of saccharides (e.g., [5]), we can fairly say that the polysaccharide core can lead to a greater stabilization of the observed membrane when compared with other structures, such as liposomes. Depending on its organization the phospholipidic environment may permit an efficient entrapment of lipophilic molecules. In this case, Biovectors would have the ability to entrap both hydrophilic and lipophilic molecules. Moreover, it would be possible to incorporate antigenic proteins on the Biovectors external surface and use them as virosomes, or as immunosomes in vaccine formulations. Some promising preliminary results have already been achieved on the entrapment and transport of interleukin-2 [6], and antigens of rabies [4], human cytomegalovirus [7] and influenza [1].

Important steps were given for the application of Biovectors; however, their structural characterization is still far from accomplished. Despite the work carried on the characterization of negative and neutral Biovectors [8], the positive systems and the problem of lipid organization have not been addressed yet. The main purpose of the present study is therefore to achieve a structural characterization (size, shape and molecular organization) of positive Biovectors, and with regard to their potential use as drug delivery systems and vaccine formulation. Light scattering is one of the most expeditious and advantageous ways to study size and shape of macromolecules in suspension (e.g., [9]). Besides being a non-destructive technique, it has the additional advantage of being applicable at fairly low concentrations. However, light scattering cannot provide information on local molecular arrangements, but only on the overall morphology of the particle. For this reason, transmission electron microscopy (TEM) was also used. Although information on the population is not easy to get from TEM, the size and shape from sample images of individual particles can be correlated with light scattering data.

2. Experimental

Biovectors.—Positive Biovectors were prepared by Biovector Therapeutics (Toulouse, France) with minor alterations to the process described elsewhere [3,6]: Maltodextrins, were incubated with NaOH and epichlorhydrin, and cationised with glycidyltrimethylammonium chloride (hydroxycholine). After neutralization, the resultant gel was disrupted by extrusion in a high pressure homogenizer (Rannie, APV, France). The polysaccharide cores obtained were purified by ultrafiltration. The addition of phospholipid (and in some cases cholesterol) was achieved by homogenization of the polysaccharide cores in the presence of a hydrated film of the desired lipids. All the samples were sterilized by filtration through 0.2 μm filters (Nalgene, Polylabo, France) and stored at 4 °C.

Apparatus.—A standard multiangle laser light scattering apparatus from Brookhaven Instruments Inc. (USA), model 2030AT was used. Light from a He–Ne laser (632.8 nm, 35 mW, Spectraphysics, model 127) was scattered by samples placed in a cylindrical cell immersed in a decalin bath with temperature control by water circulation (21.0 ± 0.5 °C). A 128 channel autocorrelator was used to compute dynamic light scattering data, yielding up to three different sampling times. The last six channels are used for baseline calculation.

Transmission electron microscopy study was carried out using a Jeol (Tokyo, Japan) Electron Microscope 100SX, operated at 60 kV.

[1] N.C. Santos, M. Prieto, and M.A.R.B. Castanho, unpublished results.

Sample preparation.—All the material used for preparation of light scattering samples was treated with chromosulfuric mixture and thoroughly rinsed with distilled water that had been previously filtered through 0.2 μm cellulose nitrate membranes (MFS, Dublin, CA). The chromosulfuric mixture removes lipid and other traces that retain dust from material wall surfaces. Samples were placed in a syringe and filtered through Millipore Millex-HV 0.22 μm disposable filter units. Retention of polysaccharide by Durapore membranes was not detected. Filtration was carried out directly into the cylindrical light scattering cells. To remove any remaining 'dust' particles from the light path an additional mild centrifugation (1300 *g* for 45 min) was performed to sediment it in the bottom of the cell. Afterwards cells were handled with extreme care. Solutions were prepared in Dulbecco's phosphate buffered saline (PBS) pH 7.4.

Electron microscopy samples were placed over copper grids, covered with a Formvar® membrane, both purchased from Sigma, and dried at room temperature. The negative staining was obtained with phosphotungstic acid solutions (1%) at different pH values.

Static light scattering.—Static light scattering (SLS) measurements were recorded according to angle and concentration. The systems studied in this work fulfil the requirements of the Rayleigh–Gans–Debye theory of light scattering [2]; such intensities were computed according to the Zimm method [10]. For practical reasons, to a good approximation:

$$\frac{Kc}{R_\theta} = \frac{1}{M_w}\left(1 + \frac{16\pi^2 n_o^2}{3\lambda^2}\langle R_g^2\rangle \sin^2\left(\frac{\theta}{2}\right) + \cdots\right) \times \left(1 + 2M_w\langle A_2\rangle c + \cdots\right) \quad (1)$$

where M_w is the weight average molecular weight, c is the concentration, θ is the scattering angle, R_g is the radius of gyration and A_2 is the second virial coefficient. $\langle R_g^2\rangle$ is also a weight averaged quantity, i.e.

$$\langle R_g^2\rangle = \frac{\sum_i w_i R_{g,i}^2}{\sum_i w_i} \quad (2)$$

[11], $\langle A_2\rangle$ is a complex average,

$$\langle A_2\rangle = \frac{\sum_i w_i^2 M_i A_{2,i}}{\sum_i w_i \sum_i w_i M_i} \quad (3)$$

[11] and K is an optical constant:

$$K = \frac{4\pi^2 n_o^2 (dn/dc)^2}{\lambda^4 N_A} \quad (4)$$

(dn/dc is the refractive index increment with concentration and N_A is Avogadro's constant). R_θ is the Rayleigh ratio, calculated relative to benzene, using (e.g., [12]):

$$R_\theta = R_{benzene,90°}\frac{n_o^2}{n_{benzene}^2}\frac{I_s}{I_{benzene}}, \quad (5)$$

I_s and $I_{benzene}$ are the intensities scattered by the sample and benzene, respectively and $R_{benzene,90°} = 11.8 \times 10^{-6}$ cm^{-1} [13].

The Zimm method is a graphical technique to extrapolate simultaneously Kc/R_θ to zero angle and infinite dilution. The data points corresponding to a given angle are extrapolated to zero concentration and, similarly, data points corresponding to a given concentration are extrapolated to zero angle. A set of the calculated points corresponds to $\theta = 0$ and A_2 can be evaluated from the slope of the concentration dependence. The other set of the calculated points corresponds to $c = 0$ and $\langle R_g^2\rangle$ can be evaluated from the slope of the angle dependence. $1/M_w$ is obtained from the intercept of both $c = 0$ and $\theta = 0$ extrapolated data.

For the sake of simplicity $\langle R_g^2\rangle^{1/2}$ and $\langle A_2\rangle$ will be referred to as R_g and A_2. Because an experimental measurement of dn/dc is prevented by the low solubility of the gel fragments, the value of the related polysaccharides was used from the tables of Huglin [14]. The dn/dc value for amylopectin, dextran and starch in water is fairly constant and equal to 0.15 cm^3 g^{-1} [14]. This is also the value for DPPC [15]. So, $dn/dc = 0.15$ cm^3 g^{-1} was set in all cases of this work.

Dynamic light scattering.—Dynamic light scattering (DLS) techniques can provide information on the dynamical properties of solutes, mainly the diffusion coefficient. The intensity of the light scattered by a small volume of the sample is recorded in the microsecond time range domain. The autocorrelation is performed afterwards. This intensity correlation func-

[2] Rayleigh–Gans–Debye theory of light scattering is valid if $|m-1| \ll 1$ and $4\pi n_o a|m-1|/\lambda \ll 1$, where $m = n_p/n_o$, n_o and n_p are the refractive indexes of the solvent and particle, respectively, a is the typical dimension of the particle and λ is the incident light wavelength in vacuum.

tion, $g_2(t)$, is related to the field correlation function, $g_1(t)$, by the Siegert relation (as long as the scattered field time function is Gaussian; [16]):

$$g_2(t) = 1 + \beta g_1(t) \tag{6}$$

where β is a constant (ideally $\beta = 1$). $g_1(t)$ is related to the solute size and shape by means of the diffusion coefficient. For small particles and also spheres of any size:

$$g_1(t) = e^{-\Gamma t} \tag{7}$$

where

$$\Gamma = Dq^2, \tag{8}$$

$$q = \frac{4\pi n_o}{\lambda} \sin\left(\frac{\theta}{2}\right), \tag{9}$$

D is the translational diffusion coefficient and can be accessed by non-linear regression techniques. If a polydisperse sample is being used, several approaches can be carried out. In this work, we have performed two kinds of data analysis: the cumulants method, proposed by Koppel [17], and Provencher's CONTIN [18]. The former provides reliable information on the statistical parameters, i.e. the moments that characterize the Γ distribution. The first and second moments, for instance, are the average and variance of Γ. However, no information on the distribution itself is obtained from cumulants. On the other hand, CONTIN provides the Γ distribution on the assumption that it is continuous. In this case:

$$g_1(t) = \int_0^{+\infty} G(\Gamma) e^{-\Gamma t} dt. \tag{10}$$

Where $G(\Gamma)$ is the intensity profile Γ distribution. $g_1(t)$ is the Laplace transform of $G(\Gamma)$. In order to evaluate $G(\Gamma)$ from $g_1(t)$ an inversion of the Laplace transform has to be carried out. CONTIN is a routine to make this inversion. Moreover, as the inversion is an ill-conditioned problem, CONTIN sets a chosen solution by considering a smoothing constraint in addition to the least squares method. The CONTIN potentialities and drawbacks were clearly tested and reviewed by Johnsen and Brown [19]. The average Γ considered for calculations is intensity averaged. The resulting averaged D is a z averaged value:

$$\langle D \rangle = D_z = \frac{\langle \Gamma \rangle}{q^2} = \frac{\sum_i w_i M_i D_i}{\sum_i w_i M_i}. \tag{11}$$

The measured D values change according to angle and concentration:

$$D = D_o\left(1 + k'_D R_g^2 q\right)(1 + k_D c) \tag{12}$$

where k'_D and k_D are constants depending on respectively the structure [20] and hydrodynamic non-ideality [21]. D_o ($\lim_{q \to 0, c \to 0} D$) is related to the hydrodynamic radius, R_h, by the Stokes–Einstein relationship:

$$D_o = \frac{kT}{6\pi\eta R_h} \tag{13}$$

where R_h is the hydrodynamic radius, k is the Boltzmann constant and η is the solvent viscosity. All the diffusion coefficients presented in this work are D_o values, although they will be referred to simply as D.

Combining SLS and DLS.—Long thin rods have a large R_g, compared to R_h. At the other extreme, homogeneous solid spheres have the smallest R_g, compared to R_h. So, the ratio R_g/R_h (usually represented by ρ) is a structure dependent parameter which usually varies from $\rho = 0.775$, for an homogeneous solid sphere, and $\rho > 2.0$, for long rigid rods. A set of ρ values according to structure can be found in [22].

Ionomers.—The polysaccharide gel fragments used in this study have several positively charged groups attached (approximately 10% molar charge/monomer residue). These fragments are therefore ionomers. Hence, it was necessary to investigate in which way the ionomer nature of gel fragments could influence the SLS and DLS measurements. The macroions tend to retard the motion of small ions, thereby giving rise to reduced diffusion coefficients for them [23]. The magnitude of the reduction depends on the ionic strength of the medium and on the ionomer charge. For sufficiently small charges of the ionomer and sufficiently high ionic strengths, the ionomer nature of the particles might not be relevant in terms of light scattering data analysis. If a relevant contribution occurred, two diffusion modes would be detected in DLS [24]. The slow mode and the total light scattered intensity would present a pronounced angular dependence [25]. Critical salt concentrations have also been reported [24]. The ionomer nature of the gel fragments and biovectors is not relevant regarding DLS data analysis because only one diffusion mode is detected in DLS, neither the slow mode nor the total light scattered intensity present a pronounced angular dependence and critical salt concentrations were not detected (I from 26.6 to 800.0 mM). So, it was not

necessary to carry out data analysis accounting for specific charge effects.

3. Results and discussion

Biovectors are microheterogeneous structures, and a progressive approach was decided for the sake of clarity. At first, the polysaccharide fragments were studied without added phospholipids. The effect of the added phospholipid on the polysaccharide fragments was studied subsequently.

The size, shape and structure of polysaccharide gel fragments.—The CONTIN and cumulants analyses are in fair agreement with each other regarding the first moment (mean) of the intensity weighted distribution of sizes. The inverse Laplace transform, performed by CONTIN reveals a unimodal, moderately polydispersed distribution (Fig. 1). The results obtained from light scattering data are presented in Table 1. In phosphate buffer, the ρ value is close to the theoretical value predicted for an impenetrable hard sphere ($\rho = 0.775$; [22]). This points to a nearly spherical geometry of the polysaccharide fragments. Transmission electron microscopy experiments provided further evidence for this idea (Fig. 2). When PBS is used, the ionic strength of the solution increases, decreasing R_g and R_h. It seems that upon increasing I, a shielding of the charged groups occurs and the polymer contracted. A decrease in the second virial coefficient supports the interpretation that the fragments become more compact. However, ρ decreases to a value lower than the value expected for a hard sphere. This surprising result can be explained by a density gradient for the scattering particles (higher in the center and lower near the surface). Other examples of non uniform density particles include microgels of polyvinylacetate [26] and β-casein micelles [20] (for review see, e.g., [27]). Conceptually, a many-arm star like polymer can also lead to results similar to the ones obtained with microgels. Entangled arms would be more compact in the inner core of the star than on the surface. A similar situation might occur with the gel fragments: the inner part of the fragment being more entangled and more similar to the macroscopic gel, and the surface more loose due to the disruption process in the Rannie homogenizer. Since the surface shell is not so compact, the polymer chains are not so entangled and they are more likely to become more sensitive to solvent interactions.

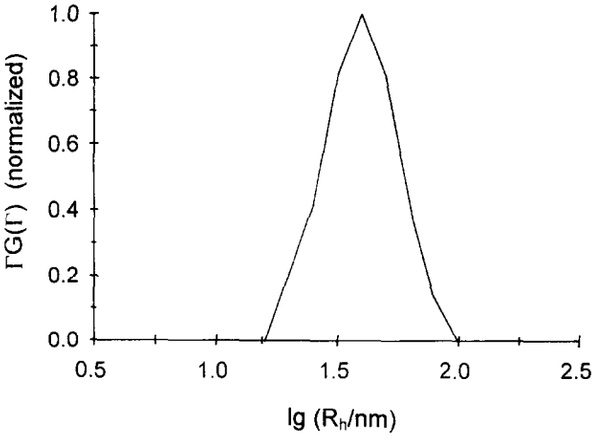

Fig. 1. Histogram executed by the method CONTIN for the dynamic light scattering results obtained with positive Biovectors with DPPC and cholesterol in PBS pH 7.4 ($\theta = 150°$, $c = 0.084$ mg/mL). The ordinate scale (normalized) results from the change of variable in Eq. (10): G was replaced by log R_h.

Fig. 2. Transmission electron microscopy photo of Positive Biovectors with DPPC, negative stained with phosphotungstic acid 1% (w/v) pH 7 (×40000). These TEM results confirm the nearly spherical geometry indicated by light scattering results.

The polysaccharide gel fragment is nearly spherical, having $R_h \approx 53.8$ nm and the structure of a microgel.

The effect of the phospholipids.—The effect of a pure phospholipid, dipalmitoylphosphatidylcholine (DPPC), and of a phosphatidylcholine mixture extracted from egg yolk (egg yolk phosphatidylcholine – EYPC) was studied. The addition of cholesterol to both lipids was also addressed (Table 1).

While EYPC does not cause dramatic changes on the polysaccharide microgel shape and dimension, DPPC causes a major increase in R_h and strong density alterations (ρ decreases). The key to these differences might be related to the fluidity of the

Table 1
Point estimates for the parameters obtained by static and dynamic light scattering for the different systems studied, in phosphate buffer and PBS (both pH 7.4). The volumic mass of the equivalent sphere (μ_{eq}) is defined as $M_w/(4/3\pi R_h^3 N_A)$. Typical relative Standard Deviations for the error distribution in the determination of the parameters are: R_h 5%, R_g 12%, M_w 10%, A_2 5%, ρ 13% and μ_{eq} 15%

Parameter	Solvent	Cores	Cores + EYPC	Cores + EYPC + chol.	Cores + DPPC	Cores + DPPC + chol.
R_h (nm)	phosphate buffer	54	61	59	84	67
	PBS	49	36	48	46	27
R_g (nm)	phosphate buffer	46	44	46	40	62
	PBS	37	50	54	50	42
$10^{-6} \times M_w$ (g mol^{-1})	phosphate buffer	5.0	11.4	13.1	4.0	14.5
	PBS	2.1	8.1	6.5	5.6	4.6
$10^4 \times A_2$ (cm^3 mol g^{-2})	phosphate buffer	−6.0	−1.8	−1.6	−13.6	−2.0
	PBS	−16.5	−1.1	−4.2	−5.9	−5.0
$\rho = R_g/R_h$	phosphate buffer	0.84	0.72	0.78	0.58	0.92
	PBS	0.69	1.38	1.14	1.09	1.56
μ_{eq} (g dm^{-3})	phosphate buffer	6.6	10.2	12.8	1.0	9.9
	PBS	3.7	35.2	12.5	12.0	49.2

lipids. At the temperature studied, DPPC bilayers are in the gel phase. On the other hand, EYPC bilayers are much more fluid due to the complex mixture of phospholipids (a tight packing of molecules is not favoured). In order to check if bilayer fluidity is a valid clue to explain the differences between the DPPC and EYPC effect, it is necessary to check if lipids are organized as bilayers in the presence of polysaccharides. Transmission electron microscopy gives the first evidence of the existence of several phospholipid bilayers surrounding polysaccharide cores. Fig. 3 (Biovectors with DPPC) was obtained from transmission electron microscopy using phosphotungstic acid to stain lipids. Several concentric bilayers shells are visible, surrounding an inner spherical core (probably the polysaccharide microgels). The thickness of such layers is in close agreement with the dimensions of a lipid bilayer [28]. Whether or not all the phospholipids are gathered in bilayers is unknown. TEM images of polysaccharide microgels alone did not reveal any of the bilayer type patterns, while they could be clearly noticed in preparations of large unilamellar vesicles of pure lipids (data not shown). A bilayer organization in both cases would imply different fluidities. It can be speculated that EYPC will probably accommodate better to the porous structure of the microgel. 'Stiff' bilayers do not 'penetrate' as much in the structure, increasing R_h.

System heterogeneity implications.—The idea of a polysaccharide core surrounded by lipid bilayers raises the question on what light scattering data analysis model one should use. The model of a simple, homogeneous sphere does not seem suitable anymore. A coated sphere has to be considered. This model consists of an internal homogeneous sphere surrounded by a concentric shell of a different refractive index (Fig. 4).

Fig. 3. Transmission electron microscopy photo of Positive Biovectors with DPPC, negative stained with phosphotungstic acid 1% (w/v) pH 7 (×240000). Multiple concentric phospholipid bilayers can be clearly noticed.

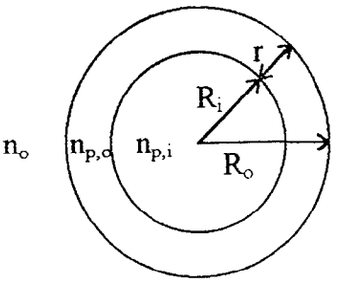

Fig. 4. Coated sphere model. An inner homogeneous sphere of radius R_i and refractive index $n_{p,i}$ is surrounded by a concentric outer shell of thickness $r = R_o - R_i$. Where R_o is the outer radius of the shell, and refractive index $n_{p,o}$. The refractive index in the medium is n_o.

The total scattered intensity per particle, I_p, can be calculated according to the Rayleigh–Gans–Debye (RGD) approximation and depends on the outer radius (R_o), on the shell thickness, on the measurement angle (by means of $x = qR_o$) and on the relative refractive indices of the coat ($m_o = n_{p,o}/n_o$) and core ($m_i = n_{p,i}/n_o$) [29]:

$$I_p = \left\{ \frac{4\pi R_o^3 (m_o - 1)}{6\pi} \left[\frac{3j_1(x)}{x} + f^3 \frac{m_i - m_o}{m_o - 1} \frac{3j_1(fx)}{fx} \right] \right\}, \quad (14)$$

$j_1(x)$ is the first order spherical Bessel function and

$$f = 1 - \frac{r}{R_o}. \quad (15)$$

Strawbridge and Hallett [30] have tried a different approach, using Lorenz–Mie theory of light scattering. A comparison of both RGD and Lorenz–Mie approaches was also carried out by Strawbridge and Hallett. The RGD approach can yield surprisingly good results, even in conditions where its assumptions are not fulfilled, except [3] when $n_i \neq n_o$ or when the coat thickness is more than 15% of R_o. The case under study in this work includes these two exceptions because the core is not water (at variance with lipid vesicles) and it might be surrounded by several bilayers of lipids. However, a more detailed inspection of Strawbridge and Hallett's results should be carried out. The basic question to be answered is:

[3] J. Watton and F.R Hallett, unpublished results.

"Are the results obtained from the Zimm method valid, in spite of the fact that we are dealing with a heterogeneous coated sphere, instead of a homogeneous sphere?" The basic equations used in the Zimm method are valid as long as $c \rightarrow 0$ and $q \rightarrow 0$ (R_g can then be obtained without assuming any model geometry). If angle and concentration dependencies are simple and smooth, extrapolations are reliable and acceptable results are obtained, even if the use of very low angles is not possible. If such dependencies are, however, complex and characterized by steep gradients, the need exists to work at a narrow range of low angles. Coated sphere light scattering intensity profiles with measurement angle, show several maxima and minima (interference pattern [30]). The number and location of these maxima and minima depend on the dimensions and refractive indices of the coated sphere. In some cases the interference pattern might not even appear, (for instance, Watton and Hallett[3] predicted a smooth decrease in the scattered light intensity with angle for $R_o = 50$ nm, $R_i = 40$ nm, $n_{p,o} = 1.45$, $n_{p,i} = n_o = 1.33$ and $\lambda = 488$ nm). In the cases tested by Watton and Hallett, for $R_o = 200$ nm and $n_{p,i} = 1.55$ (as well as $n_{p,i} = 1.39$) and $r = 10$ nm, the interference pattern was fairly smooth, with only one minimum at 80°. From 0 to 80°, the angle dependence was monotonic and smooth. Having $R_o \approx 50$ nm < 200 nm, we expect the angular dependence of polysaccharide microgel/phospholipid to be even smoother; so, reliable extrapolations in the Zimm method can be carried out. Moreover, the core refractive index must not differ very much from the refractive index of the coat ($n_{p,o} = 1.45$); that is, $m_o \approx m_i$ in Eq. (14). So, the case under study in this work might not differ much from what is expected for an homogeneous (in terms of refractive index) sphere. The results obtained by the Zimm method are still reliable and valid.

The effect of cholesterol.—Adding cholesterol to EYPC does not severely affect R_h and R_g, at variance with the effect of cholesterol in DPPC containing microgels. This is not surprising since EYPC is a complex mixture of phospholipids. Although an EYPC/cholesterol phase diagram determination is prevented by the complexity involved, it can be easily reasoned that cholesterol does not have the same impact on fluidity as it has on pure phospholipid bilayers. In liquid crystal phase bilayers, cholesterol forms domains where molecular packing is more ordered (less fluid), whilst in the gel phase cholesterol domains do not present ordered molecular packing (more fluid). If the cholesterol concentration is high enough, the cholesterol rich domains will percolate and, finally, occupy all the bilayer. In this case, all the bilayer will be in an intermediate state of fluidity, in-between liquid crystal and gel (for reviews on cholesterol action and bilayer organization see, e.g., [31]). The specific case of DPPC/cholesterol mixtures has been studied by others and a phase diagram was determined [32,33]. At the weight fraction of cholesterol used in the sample (30% w/w), and temperature of 21 °C, the system consists of two coexisting phases: a phospholipid phase and another one of phospholipid and cholesterol.

A decrease in R_h upon the addition of cholesterol to the polysaccharide microgel/DPPC systems, to an intermediate value between that obtained for DPPC and EYPC, seems reasonable since the bilayer fluidity has changed to an intermediate state. Density variations depends on the organization at the molecular level. As the events at the molecular level cannot be visualized, variations in R_g cannot be fully addressed.

4. Conclusions

Positively charged polysaccharide gel fragments obtained by disruption of a macroscopic gel appear to retain their parent gel nature. In some conditions, such fragments may not be homogeneous in terms of density. The value of the ratio $\rho = R_g/R_h < 0.775$ indicates a density gradient, higher in the fragment center and smaller near the surface. Particles with these characteristics are usually referred to as microgels. The density gradient becomes clear when the ionic strength is increased, charge repulsion is not so effective and polymer solvent interactions are more important on the surface.

The fragments shape is spherical, as detected using light scattering and TEM techniques. The hydrodynamic radius, R_h is about 50 nm (the exact value depends on the ionic strength).

As a result of the addition of phospholipids (EYPC and DPPC with or without cholesterol) to the microgels, concentric, multilamelar bilayers are formed, surrounding a polysaccharide core. However, the effects of DPPC on the size (R_h) of the scattering particles (microgel/lipid association) appear more pronounced. This difference might be related to bilayer fluidity: a more fluid bilayer, such as those formed by EYPC, would be able to accumulate more tightly to the microgel porous surface.

A polysaccharide core surrounded by lipid bilayers

seems to be suitable for drug delivery system and/or as vaccine formulations. These systems are stable, non-toxic and their size and composition are easily controlled. The microgel/lipid association could be used to entrap hydrophilic (core) or hydrophobic (lipid bilayers) drugs. The outer surface could be used to implant receptor related molecules in order to optimize targeting and delivery. An implant of antigenic molecules might also lead to virosomes.

Acknowledgements

This work was supported by Project Eureka – PUEM/S/ERC/93 and Project PECS/C/SAU/144/95 (J.N.I.C.T., Portugal). N.C.S. acknowledges a grant from J.N.I.C.T. (Portugal). The authors acknowledge the collaboration of Dr. António Pedro Alves de Matos in the transmission electron microscopy studies, and the facilities provided by the Department of Pathologic Anatomy of the Curry Cabral Hospital (Lisbon, Portugal) in the use of their microscopy equipment.

References

[1] J. Sunamoto, T. Sato, M. Hirota, K. Fukushima, K. Hiratani, and K. Hara, *Biochim. Biophys. Acta*, 898 (1987) 323–330.
[2] B. McCormack and G. Gregoriadis, *Polysialic acids: in vivo properties and possible uses in drug delivery*, in G. Gregoriadis, B. McCormack, and G. Poste (Eds.), *Targeting of Drugs 4*, Plenum Press, New York, 1994, pp. 139–145.
[3] I. De Miguel, K. Ioualalen, M. Bonnefous, M. Peyrot, F. Nguyen, M. Cervilla, N. Soulet, R. Dirson, V. Rieumajou, L. Imbertie, C. Solers, S. Cazes, G. Favre, and D. Samain, *Biochim. Biophys. Acta*, 1237 (1995) 49–58.
[4] N. Castignolles, S. Morgeaux, C. Gontier-Jallet, D. Samain, D. Betbeder, and P. Perrin, *Vaccine Res.*, in press (1996).
[5] J.H. Crowe, L.M. Crowe, J.F. Carpenter, A.S. Rudolph, C.A. Wistrom, B.J. Spargo, and T.J. Anchordoguy, *Biochim. Biophy. Acta*, 947 (1988) 367–384.
[6] N. Castignolles, D. Betbeder, K. Ioualalen, O. Merten, C. Leclerc, D. Samain, and P. Perrin, *Vaccine*, 12 (1994) 1413–1418.
[7] E. Prieur, D. Betbeder, F. Niedergang, M. Major, A. Alcover, J.-L. Davignon, and C. Davrinche, *Vaccine*, 14 (1996) 511–520.
[8] N. Santos, M. Prieto, A. Morna-Gomes, D. Betbeder and M.A.R.B. Castanho, *Biopolymers*, in press (1996).
[9] V. Bloomfield, *Ann. Rev. Biophys. Bioeng.*, 10 (1981) 421–450.
[10] B.H. Zimm, *J. Chem. Phys.*, 16 (1948) 1099–1116.
[11] N.C. Santos and M.A.R.B. Castanho, *Biophys. J.*, 71 (1996) 1641–1650.
[12] B. Chu, *Laser Light Scattering. Basic principles and practice*, Academic Press, New York, 1991, pp. 13–20.
[13] E.R. Pike, W.R.M. Pomeroy, and J.M. Vaughan, *J. Chem. Phys.*, 62 (1975) 3188–3192.
[14] M.B. Huglin, *Specific Refractive Index Increments of Polymers in Dilute Solutions*, in J. Brandrup and E.H. Immergut (Eds.), *Polymer Handbook*, John Wiley, New York, 1989, pp. VII/409–484.
[15] C.S. Chong and K. Colbow, *Biochim. Biophys. Acta*, 436 (1976) 260–282.
[16] B.J. Berne and R. Pecora, *Dynamic Light Scattering*, Robert E. Krieger Pub. Co., Malabar, 1990, pp. 62–65.
[17] D.E. Koppel, *J. Chem. Phys.*, 57 (1972) 4814–4820.
[18] S.W. Provencher, *Comput. Phys. Commun.*, 27 (1982) 213–227.
[19] R. Johnsen and W. Brown, *An Overview of Current Methods of Analysing QELS Data*, in S.E. Harding, D.B. Sattelle, and V.A. Bloomfield (Eds.), *Laser Light Scattering in Biochemistry*, Royal Society of Chemistry, Cambridge, 1992, pp. 77–91.
[20] W. Burchard, *Static and Dynamic Light Scattering Approaches to Structure Determination of Biopolymers*, in S.E. Harding, D.B. Sattelle, and V.A. Bloomfield (Eds.), *Laser Light Scattering in Biochemistry*, Royal Society of Chemistry, Cambridge, 1992, pp. 3–22.
[21] S.E. Harding and P. Johnsen, *Biochem. J.*, 231 (1985) 543–547.
[22] W. Burchard, *Static and Dynamic Light Scattering from Branched Polymers and Biopolymers*, in H.-J. Cantow, G. Dall'Asta, K. Dušek, J.D. Ferry, H. Fujita, M. Gordon, J.P. Kennedy, W. Kern, S. Okamura, C.G. Overberger, T. Saegusa, G.V. Schulz, W.P. Slichter, and J.K. Stille (Eds.), *Light Scattering from Polymers*, Springer-Verlag, Berlin, 1983, pp. 1–124.
[23] B.J. Berne and R. Pecora, *Dynamic Light Scattering*, Robert E. Krieger Pub. Co., Malabar, 1990, pp. 207–222.
[24] J. Bodycomb and M. Hara, *Macromolecules*, 28 (1995) 8190–8197.
[25] M. Sedlák and E.J. Amis, *J. Chem. Phys.*, 96 (1992) 826–834.
[26] W. Burchard and M. Schmidt, *Ber. Bunsenges. Phys. Chem.*, 83 (1979) 388–391.
[27] M. Antonietti, W. Bremser, and M. Schmidt, *Macromolecules*, 23 (1990) 3796–3805.
[28] J.M. Seddom and R.H. Templer, *Polymorphism of Lipid-Water Systems*, in R. Lipowsky and E. Sackmann (Eds.), *Structure and Dynamics of Membranes. From Cells to Vesicles*, Elsevier, Amsterdam, 1995, pp. 97–160.

[29] D.-S. Wang, H.C.H. Chen, P.W. Barber, and P.J. Wyatt, *Appl. Opt.*, 18 (1979) 2672–2678.
[30] K.B. Strawbridge and F.R. Hallett, *Can. J. Phys.*, 70 (1992) 401–406.
[31] R.A. Demel and B. de Kruyff, *Biochim. Biophys. Acta*, 457 (1976) 109–132.
[32] J.H. Ipsen, G. Karlström, O.G. Mouritsen, H. Wennerström, and M.J. Zuckermann, *Biochim. Biophys. Acta*, 905 (1987) 162–172.
[33] M.R. Vist and J.H. Davis, *Biochemistry*, 29 (1990) 451–464.